Development 137, 3047-3056 (2010) doi:10.1242/dev.052696

In vivo evidence for transdifferentiation of peripheral neurons

Melissa A. Wright[1,*], Weike Mo[2], Teresa Nicolson[2] and Angeles B. Ribera[1]

SUMMARY

It is commonly thought that differentiated neurons do not give rise to new cells, severely limiting the potential for regeneration and repair of the mature nervous system. However, we have identified cells in zebrafish larvae that first differentiate into dorsal root ganglia sensory neurons but later acquire a sympathetic neuron phenotype. These transdifferentiating neurons are present in wild-type zebrafish. However, they are increased in number in larvae that have a mutant voltage-gated sodium channel gene, *scn8aa*. Sodium channel knock-down promotes migration of differentiated sensory neurons away from the ganglia. Once in a new environment, sensory neurons transdifferentiate regardless of sodium channel expression. These findings reveal an unsuspected plasticity in differentiated neurons that points to new strategies for treatment of nervous system disease.

KEY WORDS: Dorsal root ganglia neurons, Transdifferentiation, Nav1.6, Zebrafish

INTRODUCTION

The traditional view that differentiated neurons cannot generate new cells or adopt new identities presents a substantial challenge to nervous system repair following injury. Consequently, there is great interest in identifying cells that can replace injured neurons. Current efforts focus on guided differentiation of transplanted stem cells. However, the difficulty in finding an autologous source of neural stem cells suggests the need to look for other sources of replacement cells. Relatively little is known about the potential to use a patient's own differentiated neurons for nervous system repair.

In considering which differentiated neurons might be able to repair the mature nervous system, neural crest derivatives emerge as top candidates. The neural crest comprises a unique and transient population of cells with stem cell-like properties (LaBonne and Bronner-Fraser, 1998) that generate the majority of neurons and glia in the peripheral nervous system. In addition to being self-renewing, individual neural crest cells can produce such diverse derivatives as pigment cells, neurons and glia (LaBonne and Bronner-Fraser, 1998; Le Douarin and Dupin, 2003).

Multipotent neural crest cells arise at the boundary between neural and non-neural ectoderm, then migrate throughout the embryo before differentiating into the appropriate derivatives. Recent information indicates that despite being multipotent, neural crest cells become fate-restricted during normal embryonic development (Sommer, 2001). However, transplantation to a new environment releases cells from fate restriction and allows adoption of a different fate. Raible and Eisen (Raible and Eisen, 1994) demonstrated that late-migrating neural crest cells in zebrafish embryos do not normally produce sensory neurons, even when forced to migrate early alongside the early migrating sensory neuron precursors. However, late-migrating cells acquire the ability to contribute to the sensory ganglia when early migrating neural crest cells are ablated along their migratory pathway (Raible and Eisen, 1996). Taken together, this work indicates that environmental factors can overcome fate restrictions and influence the ultimate fate decisions of individual cells. These studies further suggest that fate-restricted neural crest cells do not become committed to a particular fate until stages after migration (Raible and Eisen, 1996).

Little is know, however, about whether differentiated neural crest derivatives retain any of the plasticity of their progenitors. In vitro evidence suggests that, in both chick and mouse, embryonic dorsal root ganglia (DRG) contain cells that are capable of differentiating into sympathetic ganglia (SG) neurons (Duff et al., 1991; Paulsen and Matsumoto, 2000; Xue and Smith, 1988; Xue et al., 1985; Xue et al., 1987). The neural crest precursors of DRG and SG neurons migrate along the same path and share common progenitors. However, whereas DRG precursors stop migrating in positions adjacent to the ventral spinal cord and differentiate into glutamatergic sensory neurons, SG precursors continue to migrate until they reach the ventral notochord and differentiate into catecholaminergic autonomic neurons. Paulsen and Matsumoto (Paulsen and Matsumoto, 2000) showed that cultured embryonic mouse DRG can produce SG neurons. Interestingly, the differentiated SG neurons are found outside the DRG explant, in a ring around the periphery. On this basis, Paulsen and Matsumoto hypothesized that the embryonic DRG contains SG precursor cells, but the DRG environment inhibits autonomic differentiation. When precursor cells migrate away from the DRG they are no longer inhibited and produce autonomic neurons.

An alternative explanation for these findings is that the SG neurons arose directly from differentiated DRG neurons, rather than from a multipotent precursor cell. Specific culture conditions can induce adult rat DRG to change their morphologies and neurotransmitter phenotypes in vitro (Delree et al., 1993). It is thus

[1]Department of Physiology and Biophysics, Neuroscience Graduate Program and Medical Scientist Training Program, Anschutz Medical Campus, University of Colorado, 12800 East 19th Avenue, Mail Stop 8307, PO Box 6511, Aurora, CO 80045, USA. [2]Howard Hughes Medical Institute, Oregon Hearing Research Center and Vollum Institute, Oregon Health and Science University, Portland, OR 97239, USA.

*Author for correspondence (melissa.wright@ucdenver.edu)

Accepted 9 July 2010

possible that differentiated DRG neurons may be capable of altering their identity when placed in a new environment. However, it is not known whether differentiated neurons demonstrate such plasticity under normal physiological conditions in vivo.

We set out to test the plasticity of differentiated DRG neurons in vivo. We used the zebrafish model system, which is particularly well suited for studying changes in cell identity. External development provides easy access to embryos and larvae at stages when neurons differentiate. Furthermore, the optical transparency of the embryo and larvae, the availability of transgenic lines, and the single-cell labeling techniques allow individual cells to be followed in vivo for extended periods of time (Carney et al., 2006; Gilmour et al., 2002; Halloran and Berndt, 2003; Raible et al., 1992). Here, we use time-lapse microscopy to show that loss of the sodium channel nav1.6a leads to ventral migration of differentiated DRG neurons. Moreover, once located outside of their original ganglia, the migratory DRG neurons adopt a sympathetic-like phenotype. Our in vivo analyses indicate that differentiated sensory neurons retain the plasticity to adopt a new identity when challenged by a new environment. Furthermore, these cells exist within wild-type animals, indicating a potential endogenous source of replacement neurons within the mature nervous system.

MATERIALS AND METHODS

Animal care

Adult zebrafish (*Danio rerio*) were maintained at the Center for Comparative Medicine at University of Colorado Denver at 28.5°C on a 10-hour dark/14-hour light cycle and bred according to established procedures (Westerfield, 1995). Animal protocols were approved by the University of Colorado Committees on Use and Care of Animals. The transgenic zebrafish line Tg(–3.4neurog1:GFP)sb4 was obtained from Uwe Strahle at the University of Heidelberg (Blader et al., 2003). The Tg(elavl3:Kaede)rw0130a line was kindly provided by Hitoshi Okamoto at the Brain Science Institute, RIKEN, Japan (Sato et al., 2006). The *neurogenin* mutant line (*neurog1*$^{hi1059Tg/+}$AB) created by a transgenic insertion (Golling et al., 2002) was obtained from the Zebrafish International Resource Center (Eugene, OR, USA; NIH-NCRR P40 RR012546).

Mutant screen and positional cloning of *scn8aa*^{tW1752X}

The *scn8aa*^{tW1752X} mutant (originally named *nebula*^{tW1752X}) was first identified as an auditory/vestibular mutant from a large-scale N-ethyl-N-nitrosourea (ENU) screen (Tübingen 2000 Screen Consortium). To map the mutation, WIK wild-type fish were crossed to heterozygous carrier fish in a Tü background. Homozygous mutants were scored for loss of an acoustic startle reflex at 5 dpf, as described previously (Nicolson et al., 1998). Pooled DNA from mutants and wild-type siblings was tested using low-density genome scan simple sequence length polymorphism (SSLP) markers, which revealed linkage to chromosome 23. To narrow the critical interval, 1268 homozygous mutant larvae were used for subsequent fine mapping. The markers z14967 and z42693 defined a region of 3.2 cM containing the *scn8aa*^{tW1752X} lesion (~5.8 Mb, Zv8 assembly). Custom markers for microsatellites on contigs CR356221, CR352210, CR376824, CT573351, CR354433 and BX571776 located the mutation to a 750 kb region containing the 3′ end of the *scn8aa* gene. Sequencing of both genomic DNA and cDNA from *scn8aa*^{tW1752X} mutant larvae revealed a nonsense mutation in exon 9 of *scn8aa* gene (W1752X). Mapping primers were: CR356221_F, TGAACATCTCATGGCCTCTG; CR356221_R, GAGCAGTGCGCATTAAAACA; CR352210_F, CACACAGCACTTCAGCAAGTC; CR352210_R, TCCAACCTTTGACATGGTAGC; CR376824_F, CGGCTGCTTTCAGAGTGATTA; CR376824_R, GGCACTAAAGCGGAAGATTGT; CT573351_F, TCAGCACTGTGTGGACAGGT; CT573351_R, CGGGCAATGGGAATATATCA; CR354433_F, GGACTGCAGTGCACATAGAGA; BX571776_F, GGGGGCTGATATTTTGTCCT; BX571776_R, CCTGTCATTTTTATTGCATAAGTGC; and CR354433_R, TGAGTTTTCACACCTGCTCCT. Genotyping and sequencing primers were: Exon8_F, CAGAGGGCAGCACCATAGAT; and Exon9_R, CCAGTGCTCCACTACTGAGG.

Morpholino injections

Morpholino antisense oligonucleotides (MOs) were synthesized by Gene Tools (Philomath, OR, USA). The nav1.6a MO (1.6mo) targeted the predicted translation start methionine of nav1.6a and had 25 residues with the following sequence: 5′-GGGTGCAGCCATGTTTTCATCCTGC-3′. A second MO that targeted the splice junction between exons 3 and 4 was also synthesized (5′-ATGTGGTTTGGATCAATACTTACTC-3′). Similar results were obtained with the two different 1.6mos, and the results are pooled. Embryos injected with 1.6mo are referred to as morphants throughout this paper. Two control MOs (1.6ctl), differing from a translation blocking or splice blocking MO by five base mismatches, were synthesized. Embryos injected with 1.6ctl are referred to as controls. All MOs have been reported previously (Pineda et al., 2005; Pineda et al., 2006). MOs were injected into the yolk of one- to two-cell stage embryos at concentrations ranging between 3 and 4 ng/nl in 1% Fast Green. Inclusion of Fast Green allowed visual tracking of the injected solution.

Touch assays

The fidelity of the escape response was assessed only in embryos that were observed to swim spontaneously with a normal pattern. For each trial, the embryo was touched on the trunk with a tungsten needle and assigned a score from 0-1. A score of 1 indicated a normal response (full swimming); a score of 0.5 indicated an abnormal response (twitching, but not swimming); a score of 0 indicated no response. We performed 10 trials per embryo, resulting in a cumulative score of 0-10.

Time-lapse imaging

Live Tg(–3.4neurog1:GFP) embryos were mounted laterally in a drop of 0.5% low melting point agarose with 0.0002% tricaine on a glass-bottomed Petri dish. *Z*-stacks (15-20 images per stack; slice interval 3-4 μm) were collected every 20-30 minutes on a Deltavision Digital Devolution system running on an Olympus IX70 Inverted Microscope. DRG were imaged in embryos either at early (30-72 hpf) or later (48-96 hpf) developmental stages.

Immunocytochemistry

Whole-mount immunocytochemistry was performed as previously described with minor modifications (Svoboda et al., 2001). Briefly, embryos were fixed in 4% paraformaldehyde in PBS solution containing 0.1% Tween-20 (PBST). Fixed embryos were permeabilized by incubation in distilled H_2O followed by a 20-minute exposure to 100% acetone and a final 45-80 minute collagenase (1 mg/ml) treatment, depending upon the age of the embryo. Embryos were blocked in 10% HIGS/PBST and then incubated in 10% serum/PBST containing primary antibody. Secondary antibody was applied during a subsequent incubation. Anti-HuC/D (Molecular Probes, Carlsbad, CA, USA) was used at 1:1000; goat-anti-mouse-568 and goat-anti-rabbit-568 secondary antibodies (Molecular Probes) were used at 1:1000. For detection of GFP, the rabbit-anti-GFP-488 antibody (Molecular Probes) was used at 1:400. When used with rabbit antibodies, the anti-GFP antibody was added following extensive rinsing of the anti-rabbit secondary antibody.

We performed double immunocytochemistry for either tyrosine hydroxylase and Hu (rabbit-anti-tyrosine hydroxylase antibody, Chemicon, Billerica, MA, USA; mouse anti-HuC/D antibody) or tyrosine hydroxylase and Kaede (mouse-anti-tyrosine hydroxylase antibody, ImmunoStar, Hudson, WI, USA; rabbit anti-Kaede antibody, MBL International, Woburn, MA, USA) immunoreactivities by fixing embryos in 4% paraformaldehyde/1% DMSO. Fixed embryos were permeabilized by incubation in acetone followed by treatment with 3% H_2O_2. After blocking in 10% HIGS/PBST/1% DMSO, embryos were incubated in primary antibody. The rabbit-anti-tyrosine hydroxylase, mouse-anti-HuA, mouse-anti-tyrosine hydroxylase and rabbit-anti-kaede antibodies were used at 1:100, 1:1000, 1:50 and 1:50, respectively. Embryos were then exposed to 1:1000 goat-anti-rabbit-488 and 1:1000 goat-anti-mouse-568 in 10% HIGS/PBST/1% DMSO.

Confocal imaging and analysis of DRG position

Prior to imaging, embryos were mounted laterally in 0.5% low melting point agarose. Embryos were digitally imaged on a Zeiss LSM5 Pascal Confocal Upright Microscope. All images were obtained as *z*-stacks using either a 10× or a 40× water immersion lens.

For analysis of DRG position in live Tg(–3.4neurog1:GFP) embryos, specimens were mounted in 0.5% low melting point agarose with 0.0002% tricaine. DRG position was analyzed throughout the length of the embryo using a Zeiss LSM5 Pascal Confocal Upright Microscope. GFP^+ DRG cells were considered to be ectopic if they resided more than one cell body length ventral to the spinal cord-notochord boundary.

Cell tracking and photoconversion of Kaede

48 hpf live Tg(elavl3:Kaede) embryos were mounted laterally on their right side as described above. Individual DRG neurons were photoconverted from green to red on a Zeiss LSM5 Pascal Confocal Upright Microscope by focusing 405 nm light onto a 4×4 pixel spot for 3 seconds with 3% laser intensity. Approximately four DRG neurons were photoconverted in each embryo. Every other day, photoconverted cells were re-illuminated as described above to convert newly synthesized protein. Following photoconversion and imaging, embryos were released from the agarose and maintained at 28.5°C. When embryos were fixed for immunocytochemistry following cell tracking, Kaede was photoconverted to red throughout the embryo using blue light on an epifluorescent microscope.

Single-cell electroporation

Live 4 dpf Tg(–3.4neurog1:GFP) embryos were mounted laterally in 0.5% low melting point agarose with 0.0002% tricaine. A small incision was made in the dorsal skin to facilitate insertion of the electrode with minimal disruption to the sensory processes innervating the skin. GFP^+ DRG neurons were electroporated by placing an electrode filled with 300 μM Alexa-568 dye adjacent to the target cell and stimulating for 20 mseconds with a 4-5 μA pulse (Stimulus Isolator, WPI A360, Sarasota, FL, USA). Following electroporation, embryos were released from the agarose and incubated with antibiotics.

Statistical analysis

All statistical analyses were performed using InStat software (GraphPad Software, La Jolla, CA, USA). For single comparisons, unpaired two-tailed *t*-test was used; for multiple comparisons, ANOVA analysis was performed with post-hoc correction. The specific tests used for each analysis were determined based upon whether the data fit a parametric curve or not and are indicated in the text. For all graphs, the data are presented as mean ± s.e.m.

RESULTS

Loss of nav1.6 results in inappropriately located DRG neurons

We first characterized the position of DRG neurons in nav1.6 knock-down and control embryos. In studies characterizing zebrafish DRG and SG development, An et al. (An et al., 2002) occasionally found cells that appeared to be DRG neurons ectopically positioned between the typical location of the DRG and the SG, which led them to suggest the possibility of a secondary migration of differentiated neurons from the DRG to the site of the SG. Similarly, we observed an increase in the number of ectopically positioned DRG neurons upon knock-down of the nav1.6a sodium channel (Fig. 1).

To easily identify DRG neurons, we used a Tg(–3.4neurog1:GFP) transgenic line that expresses GFP in RBs, spinal interneurons and differentiating DRG neurons (Blader et al., 2003). We knocked down the nav1.6 sodium channel using well-characterized morpholinos (Pineda et al., 2005; Pineda et al., 2006). GFP^+ DRG cells localized in a stereotypic pattern adjacent to the ventral spinal cord in 2, 3 and 4 dpf control embryos (normal position; Fig. 1A). As previously described (An et al., 2002), we found a small number of DRG cells in more ventral positions adjacent to the notochord (ectopic position; Fig. 1C). Overall,

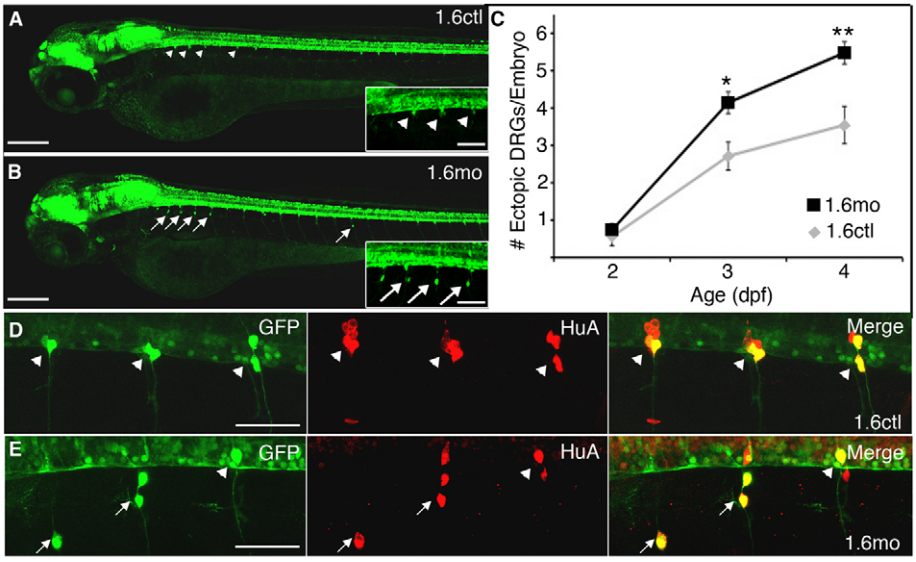

Fig. 1. DRG neurons reside in abnormal positions in nav1.6 morphants. (**A**) GFP^+ DRG neurons show a stereotypic pattern and localize to the ventral boundary of the spinal cord (arrowheads) in each trunk hemisegment of control 3 dpf Tg(ngn:GFP) embryos. (**B**) By contrast, many GFP^+ DRG cells reside in more ventral locations (arrows) in 1.6 morphants. Insets in A and B show segments 2-5 at higher magnification. (**C**) In both controls (gray diamonds) and morphants (black squares) the average number of ectopic DRG neurons per embryo increases between 2 and 4 dpf. Additionally, a larger number of ectopic DRG neurons are found in morphants than controls at 3 and 4 dpf (*P<0.01 versus 1.6mo; **P<0.001 versus 1.6mo; Kruskal-Wallis nonparametric ANOVA). (**D**) In 4 dpf control embryos, DRG neurons (arrowheads) express both GFP (green) and HuA (red), a marker of neuronal differentiation. (**E**) Ectopic DRG neurons (arrows) are also positive for both GFP and the neural differentiation marker, HuA. Embryos are mounted laterally, with anterior towards the left and dorsal at the top for all figures. Scale bars: 200 μm in A,B (70 μm in insets); 50 μm in D,E.

morphant embryos showed the typical pattern of localization of GFP$^+$ DRG cells adjacent to the ventral spinal cord. However, in comparison with control embryos, morphants had a significantly larger number of ectopic GFP$^+$ DRG cells (Fig. 1B,C). Although we saw ectopic GFP$^+$ DRG cells more frequently in the anterior segments, nav1.6a knock-down increased the incidence of ectopic DRG cells similarly throughout the embryo (see Fig. S1 in the supplementary material).

The Tg(–3.4neurog1:GFP) line that we used commences transgene expression in DRG precursors as they initiate differentiation into sensory neurons, but before they assume a neuronal morphology (McGraw et al., 2008) (data not shown). It is therefore feasible that ectopic GFP$^+$ DRG cells fail to complete neuronal differentiation and either remain undifferentiated or adopt a glial fate, as is the case for ectopic DRG precursors in the absence of neurogenin 1 (McGraw et al., 2008). To determine whether GFP$^+$ ectopic DRG cells maintain a neuronal identity, we immunostained 4 dpf nav1.6 morphant and control Tg(–3.4neurog1:GFP) embryos for HuA, a marker of neuronal differentiation. We found that both normally positioned and ectopic GFP$^+$ DRG cells expressed HuA (Fig. 1D,E). Furthermore, similar to normally positioned DRG neurons, ectopic DRG cells extended axons dorsally and ventrally. The data indicate that displaced DRG cells express markers of differentiated neurons, despite their atypical location.

Ectopic DRG neurons migrate ventrally after they extend axons

In zebrafish, neural crest precursors of DRG neurons migrate ventrally past the ventral spinal cord, backtrack dorsally and initiate post-mitotic differentiation upon reaching the stereotypic position of the DRG (Raible et al., 1992). Other neural crest cells continue to migrate ventrally and give rise to other neuronal populations, such as the sympathetic ganglia and the enteric nervous system (Raible et al., 1992). One possible explanation for the ventral position of ectopic DRG neurons is that their neural crest precursors continue to migrate ventrally past the ventral spinal cord, but do not backtrack dorsally. However, the number of displaced DRG neurons did not differ between controls and morphants at 2 dpf (Fig. 1C), a time when many DRG precursors would be expected to have differentiated (An et al., 2002). This finding suggests the alternative explanation that DRG precursors migrate normally, reach their stereotypic location adjacent to the ventral spinal cord and differentiate. Subsequently, a subset of differentiated DRG neurons undergoes a novel second ventral migration.

We performed time-lapse imaging of Tg(–3.4neurog1:GFP) morphants and controls to determine whether ectopic DRG neurons arise from abnormal migration of their neural crest precursors or from a second ventral migration. All 114 GFP$^+$ DRG cells imaged were present at the stereotypic location of DRG neurons adjacent to the ventral spinal cord upon initiation of GFP expression (Fig. 2A,B; left column). Moreover, all DRG precursors differentiated into neurons at this location on the basis of extension of dorsal and ventral axons. However, some DRG neurons translocated their somata to ectopic positions after extending axons (Fig. 2B). Consistent with our previous results (Fig. 1), more DRG neurons migrated ventrally in morphant than control embryos. These data reveal that ectopic DRG neurons migrate to a new position only after they differentiate. On this basis, we refer to ectopically positioned DRG as migratory DRG neurons.

Migratory DRG neurons morphologically resemble sympathetic neurons

To determine where migratory DRG neurons ultimately reside, we followed individual cells to later stages using the Tg(elavl3:Kaede) line. In this line, Kaede can be detected in DRG neurons through 13 dpf. Furthermore, the photoconvertible properties of the Kaede fluorescent protein allow selection of individual cells that can then be followed in vivo for longer periods of time than are feasible using time-lapse methods. At 2-3 dpf, we used UV illumination to photoconvert Kaede from a green to a red fluorescent protein in individual DRG neurons in nav1.6 morphant embryos (Fig. 3A). At 11 dpf, 20% of migratory DRG neurons (11/56) had reached the region of the ventral notochord, the location of the sympathetic ganglia (Fig. 3B). Interestingly, we did not observe any migratory DRG neurons at positions ventral to the sympathetic ganglia, where enteric neuron precursors would be found. Consistent with these findings, we found an increased number of TH$^+$/HuA$^+$ neurons in the region of the sympathetic ganglia in 11 dpf nav1.6 morphant embryos compared with controls (Fig. 3C). Interestingly, 1.6mo did not increase the number of TH$^+$/HuA$^+$ neurons within the sympathetic ganglia in *neurogenin* mutants, which lack DRG neurons (Fig. 3C), suggesting that DRG neurons provided the increased number of SG neurons present in nav1.6 morphants.

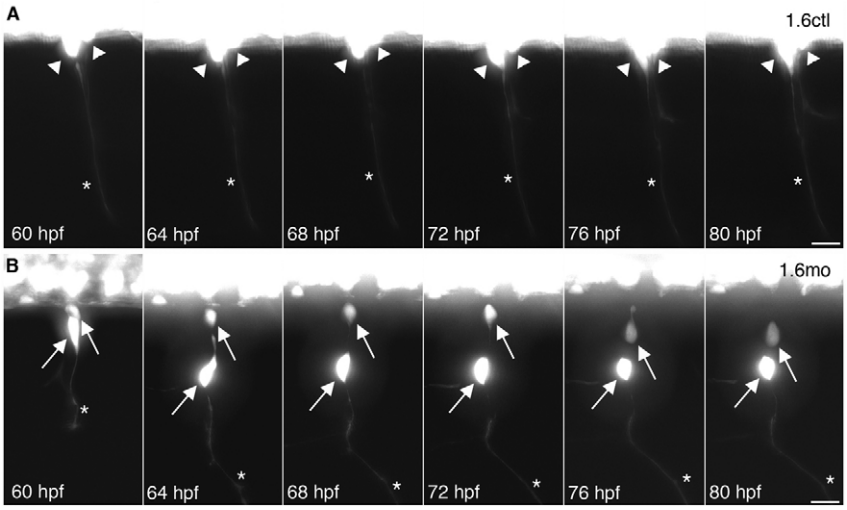

Fig. 2. DRG neurons migrate to abnormal ventral positions after they have extended axons. (**A**) Two adjacent DRG neurons (arrowheads) in a Tg(–3.4neurog1:GFP) control embryo extended axons (asterisk) by 60 hpf. Between 60 and 80 hpf, control DRG neurons maintain their position and remain lateral to the ventral spinal cord. Data are representative of 16 control DRG that were followed by time-lapse imaging. (**B**) In a 60 hpf Tg(–3.4neurog1:GFP) morphant embryo, DRG neurons (arrows) reside lateral to the ventral spinal cord and have extended axons (asterisks), similar to the control shown in A. However, at 64 hpf, one DRG neuron has migrated ventrally. By 76 hpf, the second DRG neuron has also migrated ventrally. Data are representative of 18 ventrally migrating morphant DRG neurons. Scale bars: 20 μm.

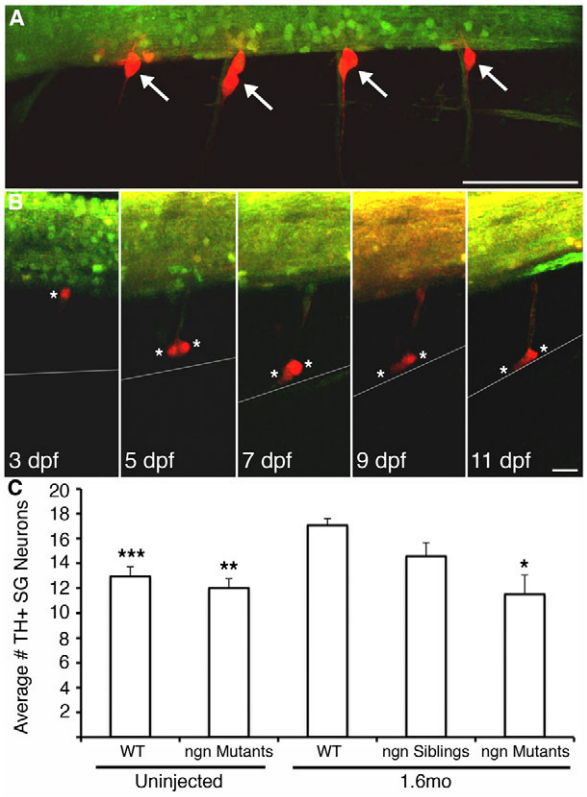

Fig. 3. Migratory DRG migrate as far ventrally as the location of the sympathetic ganglia. (**A**) Transgenic expression of photoconvertible Kaede in DRG allows identification of progeny and migratory paths. At 60 hpf, DRG (white arrows) in four hemisegments of a nav1.6 morphant Tg(elavl3:Kaede) embryo were selectively illuminated with UV light, as evidenced by photoconversion of Kaede from a green fluorescent molecule to red in DRG, but not nearby spinal cord, neurons. (**B**) At 3 dpf, a single DRG neuron (white asterisk) shows a stereotypic location at the ventral boundary of the spinal cord. At 5 dpf, the cell divides into two cells (white asterisks), but retains its axon, then migrates ventrally. At 7 dpf, both cells approach the ventral boundary of the notochord (grey line), the location of the sympathetic ganglia. The two migratory DRG cells remain in the region of the sympathetic ganglia at subsequent times (e.g. 11 dpf). (**C**) Consistent with migration of DRG neurons to the location of the sympathetic ganglia, the number of TH^+ neurons in the sympathetic ganglia at 11 dpf is significantly greater in 1.6 morphant embryos compared with wild type (***P<0.001 versus 1.6mo wild type, nonparametric ANOVA). However, injection of 1.6mo does not produce an increase in TH^+ neurons in the sympathetic ganglia in *neurogenin* mutants, which lack DRG neurons (**P<0.01 versus 1.6mo wild type; *P<0.05 versus 1.6mo wild type; Kruskal-Wallis nonparametric ANOVA. Scale bars: 30 μm in A; 15 μm in B.

Using photoconvertible Kaede (Fig. 3), we found that migratory DRG neurons travel as far ventrally as the location of the sympathetic ganglia. Ectopic DRG neurons will experience a different environment than those in the typical location. To determine whether migratory DRG neurons acquire characteristics of sympathetic neurons, we first examined morphology by electroporating low molecular weight Alexa568 into GFP^+ DRG neurons of live 4 dpf Tg(–3.4neurog1:GFP) embryos. At 5 dpf, normally positioned DRG neurons showed a stereotypic bipolar morphology in both morphant and control embryos, i.e. DRG neurons extended axons dorsally into the spinal cord and ventrally toward skin or muscle (Fig. 4A,B). By 7 dpf, existing axons underwent extensive branching, but no new processes emerged from the soma (Fig. 4A,B). Migratory DRG neurons maintained their dorsal and ventral axons. However, they also sprouted novel lateral processes directly from their somata (Fig. 4C). The length and number of these lateral fibers increased with age (data not shown).

Electrical activity has been shown to regulate neurite outgrowth (Fields et al., 1990; Nasevicius and Ekker, 2000). Consequently, sprouting of lateral processes by migratory DRG neurons may result directly from nav1.6a knock-down, rather than from the new environment encountered by the ectopic cells. If so, we would expect to see a difference in the number of lateral processes displayed by migratory DRG neurons in control versus morphant embryos. Alternatively, if the new environment of migratory DRG neurons encourages sprouting of lateral processes from the soma, we would not expect to see a difference in the number of lateral processes generated by migratory DRG in controls versus morphants. Analysis of lateral processes indicated that the position of the DRG soma, rather than the nav1.6a status of the embryo, predicted sprouting of lateral processes (Fig. 4E). Moreover, migratory DRG neurons sprout lateral processes with a morphology and pattern (Fig. 4C, right column) that is reminiscent of the morphology of another neural crest derivative, sympathetic ganglia neurons (Fig. 4D), which is consistent with adoption of a new identity.

Migratory, but not normally-positioned, DRG neurons express tyrosine hydroxylase

Sympathetic ganglia differ from DRG neurons not only with respect to morphology, but also in neurotransmitter phenotype. By 10 dpf, the majority of sympathetic neurons express tyrosine hydroxylase (TH), an enzyme required for synthesis of catecholamine neurotransmitters. However, by 10 dpf, morpholinos undergo substantial turnover, resulting in poor protein knock-down (Nasevicius and Ekker, 2000). To avoid this potential difficulty, we identified a nonsense mutation in the *scn8aa* gene. The mutant was isolated on the basis of loss of the larval acoustic startle reflex at 5 dpf. Subsequent mapping of the mutation and genomic DNA sequencing revealed a single base substitution in exon 9 that changed a tryptophan codon to a nonsense one (Fig. 5). This mutation is very similar to the $scn8a^{medtg}$ allele, which produces a null mutation (Meisler et al., 2004).

To test the suitability of the nav1.6a mutant for our studies, we compared the mutant phenotype with phenotypes previously described in nav1.6 morphants (Pineda et al., 2005). Pineda et al. (Pineda et al., 2005) previously found that morpholino knock-down of nav1.6a reduced touch sensitivity of 2, 3 and 5 dpf morphant embryos compared with controls. Whereas Rohon-Beard sensory neurons initially mediate the touch response, DRG neurons begin to support this function at stages beyond 3 dpf. We found that mutants and morphants displayed similarly reduced touch sensitivities as late as 8 dpf, when the majority of Rohon-Beard cells have undergone cell death (Svoboda et al., 2001) (Fig. 6A). Thus, the data support deficient DRG function in both morphants and mutants.

We next compared the number of migratory DRG neurons in nav1.6 mutants versus morphants. As expected, nav1.6 mutants had an increased number of migratory DRG neurons compared with sibling embryos (Fig. 6B,C,D). Interestingly, 4 dpf mutants also had an increased number of migratory DRG neurons compared with morphants (Fig. 1C, Fig. 6B; P<0.001 versus morphants), consistent with a more complete knock-down of the channel protein. The

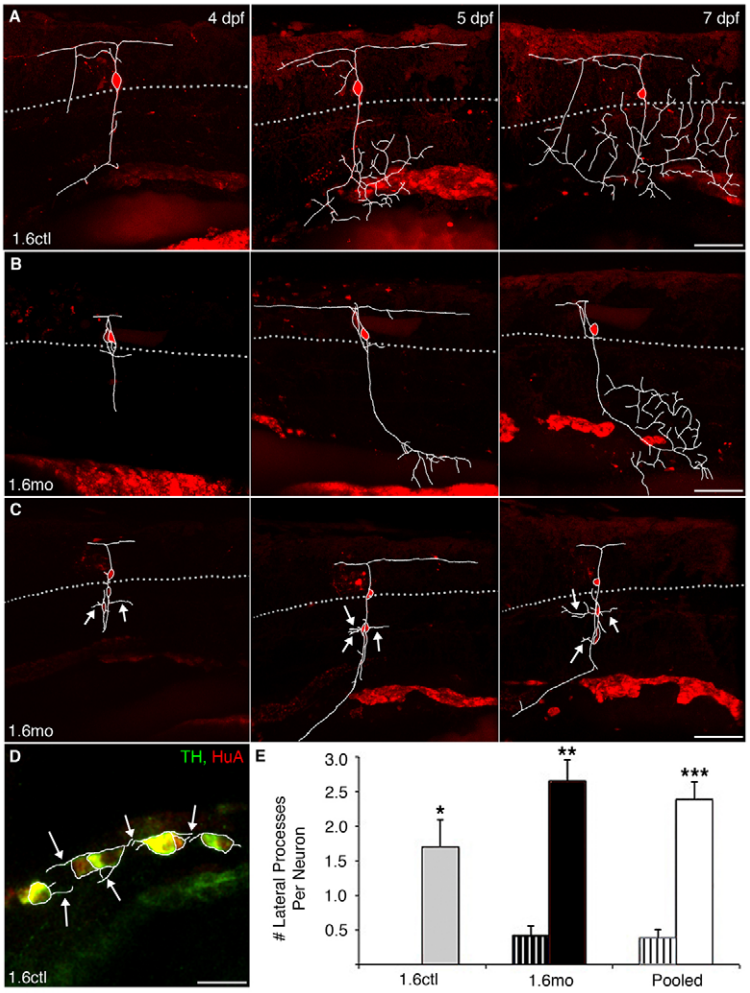

Fig. 4. Migratory DRG neurons sprout novel lateral processes. DRG neurons were electroporated with Alexa568 at 4 dpf and followed to 7 dpf. In panels A-C, dye-labeled DRG processes were traced in white from individual slices and overlaid onto the projected images. The dotted gray line represents the ventral boundary of the spinal cord, where DRG are typically found. (**A**) In a control embryo, a DRG neuron extends a single process ventrally at 4 dpf. At subsequent times, the process begins to branch once it reaches more ventral positions. (**B**) In a nav1.6 morphant embryo, a correctly positioned DRG neuron also extends a ventral process that branches. (**C**) By contrast, ectopic DRG neurons of morphant embryos sprout processes (white arrows) that emanate from the soma and extend laterally. (**D**) In an 11 dpf control embryo, laterally projecting processes emerge from the soma of TH^+/HuA^+ sympathetic neurons (white arrows). (**E**) Normally positioned DRG neurons (striped bars), in either control (grey) or morphant (black) embryos, sprout few or no laterally projecting processes from their soma. By contrast, migratory DRG neurons (solid bars) display many more laterally projecting processes (**P*<0.05 versus normally-positioned 1.6ctl; ***P*<0.001 versus normally-positioned 1.6mo; ****P*<0.001 versus normally positioned pooled cells; Kruskal-Wallis nonparametric ANOVA). White bars represent pooled morphant and control cells. Scale bars: 60 μm in A-C; 20 μm in D.

increase in the number of migratory DRG neurons in nav1.6 mutants versus siblings was found at both 4 and 13 dpf (Fig. 6B). These findings support the use of the nav1.6 mutant to examine TH expression in migratory DRG neurons at stages beyond 10 dpf.

In 13-15 dpf larvae, we classified HuA^+ neurons in segments 2-6 as normally positioned DRG, as migrating DRG or as SG neurons based on the position and shape of the soma (Fig. 7A-G). As expected, we did not detect TH in normally positioned DRG in either nav1.6 siblings or mutants (TH^+: 1/782 and 0/271 neurons, respectively). By contrast, ~90% of sibling and mutant sympathetic ganglia neurons (531/607 and 210/230 neurons, respectively) expressed TH (Fig. 7J). Taken together, the data indicate that loss of nav1.6 does not alter the normal expression pattern of TH in DRG or SG neurons.

We next examined migratory DRG neurons for TH expression. In both sibling and mutant larvae, 25% of migratory DRG neurons expressed TH (54/213 and 27/118 neurons, respectively). Importantly, the proportion of migratory DRG neurons that

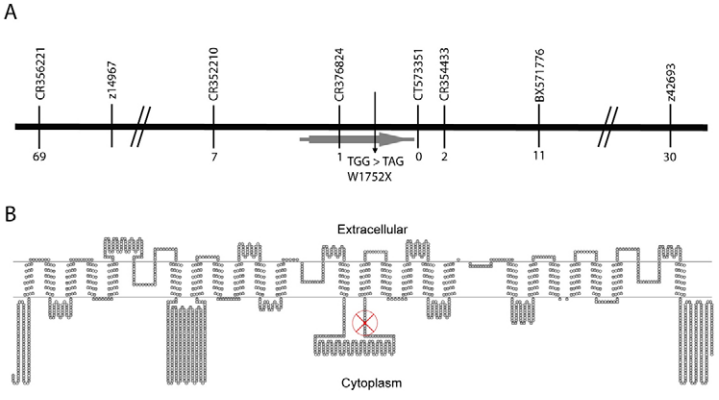

Fig. 5. Genetic map and identification of the *scn8aa*^{tW1752X} mutation. (**A**) A genetic map near the *scn8aa*^{tW1752X} locus on zebrafish linkage group 23. Two known SSLP markers from MGH panel and six customized markers are shown. A total of 1268 larvae from 10 mapping crosses were examined with the markers, except z14967, and the number of recombinants is indicated below the markers. For z14967 marker, two recombinants were found in 157 larvae tested. The gray arrow below the chromosome line indicates the *scn8aa* gene and the arrow across the chromosome line represents the *scn8aa*^{tW1752X} mutation. (**B**) A topographic diagram of the Nav1.6a channel secondary structure. The channel consists of four major subunits with six transmembrane segments. The *scn8aa*^{tW1752X} lesion is indicated by a circle between the 12th and 13th transmembrane domain.

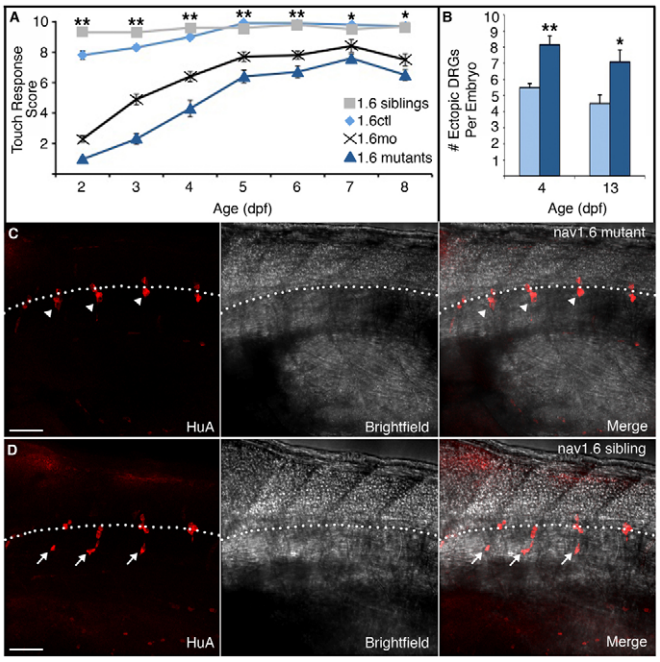

Fig. 6. nav1.6 mutants recapitulate the morphant phenotype. (**A**) nav1.6 morphants (black crosses) and mutants (dark-blue triangles) show a severe reduction in touch sensitivity at 2 dpf compared with control (gray squares) and sibling (light blue diamonds) embryos. Although nav1.6 morphants and mutants partially recover by 5 dpf, they show similar deficits in touch sensitivity that persist as late as 8 dpf (**P<0.001 for nav1.6 siblings and controls versus nav1.6 mutants and morphants; **P<0.01 for nav1.6 siblings and controls versus nav1.6 mutants and morphants; Kruskal-Wallis nonparametric ANOVA). (**B**) The increase in the number of ectopic DRG neurons in nav1.6 mutant versus control larvae persists to 13 dpf (**P<0.0001, *P=0.0105; Mann-Whitney test). Scale bars: 50 μm. (**C**) Additionally, whereas HuA-positive DRG neurons cluster lateral to the ventral spinal cord in nav1.6 siblings (arrowheads), (**D**) many individual DRG neurons in nav1.6 homozygous mutants are located ectopically, in more ventral positions (arrows) reminiscent of DRG position in nav1.6 morphants. The broken white line indicates the ventral boundary of the spinal cord.

expressed TH was not affected by genotype (Fig. 7J), suggesting that TH expression is a function of the migratory DRG phenotype rather than the result of nav1.6a knock-down. To determine whether Hu^+/TH^+ cells that we classified as migratory DRG neurons originated from DRG neurons rather than from neurons from another location (e.g. the SG), we followed differentiated DRG neurons in Tg(elavl3:Kaede) embryos and subsequently examined them for TH expression. We identified migratory DRG neurons in 5 dpf larvae on the basis of Kaede expression (the elavl3 promoter does not drive expression of Kaede in SG neurons at this time), position and the characteristic bipolar DRG morphology. Photoconverted DRG neurons were tracked until 11 dpf, at which time we processed larvae for Kaede and TH immunoreactivites. Consistent with our classification of Hu^+/TH^+ cells located between the spinal cord and the notochord as migratory DRG neurons, we found $Kaede^+/TH^+$ cells that we had previously identified as DRG neurons. In summary, nav1.6a reduction increases the number of migratory DRG neurons. However, regardless of their nav1.6 status, migratory DRG neurons acquire new properties that are hallmarks of SG neurons.

DISCUSSION

Although many in vitro studies suggest the presence of bipotent precursor cells within the DRG (Duff et al., 1991; Paulsen and Matsumoto, 2000; Xue and Smith, 1988; Xue et al., 1985; Xue et al., 1987), our work demonstrates that differentiated DRG neurons retain a remarkable degree of plasticity in vivo. Using the zebrafish model system, we identified cells that first acquire positional, morphological and molecular properties of differentiated DRG neurons. However, they later migrate out of the ganglion, while maintaining two markers of neuronal differentiation: Hu immunoreactivity and axons.

We found migratory DRG neurons in wild type as well as nav1.6 morphant and mutant embryos. However, about 20% of wild-type behaviorally normal embryos do not have migratory DRG neurons, suggesting that migratory DRG neurons do not represent a distinct neuronal population with an essential function. The ventral trajectory of the migration pathway towards the sympathetic ganglia raises the possibility that these former residents of the DRG seek the sympathetic ganglia as a new environment. Consistent with this possibility, we found that migratory DRG neurons not only acquire positions similar to those of sympathetic ganglia, but also molecular and morphological characteristics of differentiated sympathetic neurons.

Although the traditional view of cellular differentiation implies irreversible commitment to a given cell identity, recent work indicates that differentiated cells can adopt a new identity, i.e. transdifferentiate (Dupin et al., 2000; Dupin et al., 2003; Jee et al., 2010; Kanazawa et al., 2010; Lu et al., 2010; Rizvi et al., 2002; Roberson et al., 2004; Shang et al., 2010; Yin et al., 2010; Yoshii et al., 2007). Indeed, transdifferentiating cells have been found in the endocrine pancreas (Lu et al., 2010), the auditory system (Roberson et al., 2004; Shang et al., 2010), the retina (Yoshii et al., 2007), adipose tissue (Jee et al., 2010) and the sympathetic nerves (Kanazawa et al., 2010) in diverse vertebrate species such as amphibia (Yoshii et al., 2007), avia (Roberson et al., 2004; Shang et al., 2010), rodents (Kanazawa et al., 2010; Lu et al., 2010) and humans (Jee et al., 2010; Yin et al., 2010). The wide-ranging distribution of the evidence for transdifferentiation across tissues and organisms warrants a re-examination of our definition of differentiation to include the possibility of a plastically differentiated state.

In some situations, cells acquire a new fate by first dedifferentiating into a precursor-like cell that divides to produce multiple types of progeny (Dupin et al., 2000; Dupin et al., 2003; Jee et al., 2010). In our studies, migratory cells first appeared after DRG differentiation had initiated, as assessed by Hu expression and axon extension. In time-lapse experiments (Fig. 2), eight migratory cells had clearly visible axons at the onset of migration. Six of these did not divide, suggesting that cell division is not a requirement for expression of a sympathetic phenotype. In the other two instances, when DRG number increased in a hemisegment, the DRG cells did not round up and retract their axons, suggesting that dedifferentiation did not occur prior to cell proliferation, as reported previously (An et al., 2002). Overall, our data support direct transdifferentiation of one cell type to another in the sensory system, as has been shown in the regenerating auditory system (Roberson et al., 2004; Shang et al., 2010).

If the differentiated state is plastic, how do cells maintain their identity? In the case of plastically differentiated DRG neurons, one possibility is that the local DRG environment either actively maintains differentiation of DRG neurons or inhibits differentiation of SG neurons. This is supported by the finding that in both our

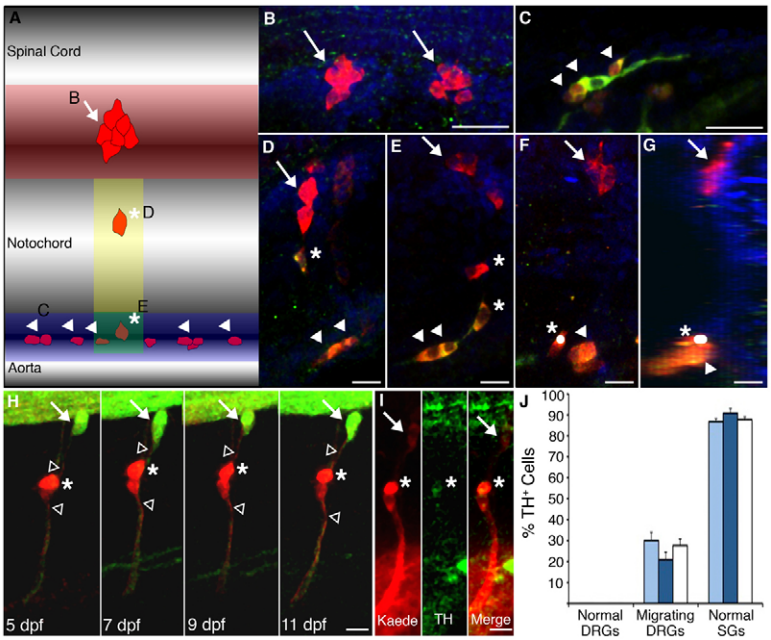

Fig. 7. Migrating DRG neurons express TH, a marker of the sympathetic ganglia. (**A-G**) HuA$^+$ neurons were classified as normally positioned DRG neurons (red shaded region; B, arrows), SG neurons (blue shaded region; C, arrowheads), or migratory DRG (yellow and green shaded regions; D-G, asterisks indicate migratory cells and arrowheads SG neurons). The yellow and green regions are both directly ventral to the normal location of the DRG; cells in the green region were classified as migratory DRG and not SG if they were positioned dorsal to nearby SG neurons and/or were elongated along the dorsoventral axis. (F) A projection of a confocal *z*-stack image shows a TH$^+$ neuron identified as a migratory DRG neuron (asterisk, white dot), based upon its vertical orientation, adjacent to a sympathetic neuron (arrowhead). The projection consisted of 20 confocal slices obtained in increments of 3 μm. (G) Rotation of the projected image shows that the migratory DRG neuron (asterisk) resides within the sympathetic ganglia. (**H**) In Tg(elavl3:Kaede) larvae, we photoconverted two migratory DRG neurons (red, asterisk), identified by Kaede expression and the presence of dorsal and ventral axons (unfilled arrowheads) at 5 dpf, and followed them to 11 dpf. The white arrow indicates a normally positioned DRG that was not photo-converted and remains green fluorescent. (**I**) At 11 dpf, one of the cells was positive for both Kaede (red) and TH (green) immunoreactivities (asterisk). Overall, 25% of photoconverted DRG neurons (6/24; 15 embryos) showed TH immunoreactivity. (**J**) In 13-15 dpf larvae, normally positioned DRG neurons (B) rarely express TH. By contrast, the majority of SG neurons (C) do express TH. A significant number of migratory DRG neurons (D,E) express TH. However, the genotype of the embryo did not affect the percent of TH$^+$ normally positioned DRG, SG or migratory DRG (light-blue bars, nav1.6 siblings; dark-blue bars, nav1.6 mutants; white bars, all embryos pooled regardless of genotype). (B-G) Embryos were immunostained for HuA (red) and TH (green); Hoescht (blue)-labeled nuclei. Scale bars: 20 μm in B,C; 10 μm in D-G; 12.5 μm in H,I.

studies and Paulsen and Matsumoto's studies on mouse DRG explants (Paulsen and Matsumoto, 2000), TH$^+$ neurons were generated by cells that migrated away from the DRG and not within the DRG itself. Similarly, Rizvi et al. (Rizvi et al., 2002) suggested that the endoneurium maintains Schwann cell differentiation, as Schwann cells that escape the endoneurium in peripheral nerve injury revert to a bi-potent progenitor cell phenotype. Although the importance of local cues in directing differentiation has long been known (Gurdon et al., 1993; Sommer, 2001), these studies indicate that cell position can be a critical regulator of identity in differentiated, as well as differentiating, cells.

As mentioned, 80% of wild-type zebrafish larvae have a small number of migratory DRG neurons, and 64% of wild-type larvae have migratory DRG neurons that morphologically and molecularly (TH expression) resemble SG neurons. This finding indicates that conversion of DRG neurons to SG neurons can occur under normal physiological conditions so long as DRG neurons escape their normal environment. We propose that loss of nav1.6a increases escape of DRG neurons from the ganglion, which in turn releases them from identity restriction. This is consistent with our finding that the number of migratory cells increases in embryos lacking nav1.6a, but the percent of migratory cells (~25%) that express TH does not. Curiously, migratory DRG neurons express TH regardless of whether they reach the location of the sympathetic ganglia, suggesting that differentiation into SG neurons results from disinhibition of the phenotype rather than inductive cues within the SG. It is not clear at this point whether all migratory DRG neurons ultimately differentiate into SG neurons or whether some retain their DRG phenotype.

We found that about 25% of migratory DRG neurons expressed TH immunoreactivity by 13-15 dpf. It is possible that the remainder of the migratory DRG neurons might either maintain their DRG identity or acquire TH immunoreactivity at later developmental stages that we did not examine. Alternatively, these neurons might lose glutamate expression and acquire the ability to synthesize a non-adrenergic transmitter. Future studies will address these interesting possibilities and test whether migratory DRG neurons can transdifferentiate into cells other than sympathetic ganglion neurons.

It is somewhat surprising that a voltage-gated sodium channel has such a profound impact on the migratory behavior of neurons. However, electrical activity regulates diverse developmental events, such as cell death and survival (Svoboda et al., 2001), interneuron differentiation (Borodinsky et al., 2004; McDearmid et al., 2006), axon guidance (Hanson and Landmesser, 2004) and cell-adhesion molecule expression (Itoh et al., 1997; Stevens et al., 1998). Consequently, loss of nav1.6a may alter cell-adhesion molecule expression in DRG neurons, resulting in increased migratory behavior. This possibility is particularly appealing as DRG neurons within the ganglia often fail to adhere to each other in nav1.6a morphants and mutants (data not shown). Additionally, studies using cultured mouse DRG demonstrated that specific frequencies of electrical activity differentially regulate expression of cell-adhesion molecules (Itoh et al., 1997; Stevens et al., 1998). Loss of a voltage-gated sodium channel could change the frequency of electrical activity and thereby lead to altered cell adhesion molecule expression. Alternatively, loss of a sodium channel alpha subunit may affect beta subunits, which can act as cell-adhesion molecules (Fein et al., 2008; Malhotra et al., 2000; McEwen and Isom, 2004).

A recent study by Perrson et al. (Perrson et al., 2009) showed a correlation between downregulation of Nav1.6 and behaviors associated with neuropathic pain in mouse peripheral nerve injury models. Interestingly, the presence of sympathetic fibers within the

DRG in several neuropathic pain models implicates inappropriate activation of pain fibers by sympathetic neurons as a mechanism of neuropathic pain (Chien et al., 2005; Chung and Chung, 2001; Kim et al., 1999; Shinder et al., 1999; Zhang and Strong, 2008). However, little is known about the mechanism of sympathetic sprouting within the DRG. Our work suggests that downregulation of Nav1.6 may allow neurons to escape the DRG following nerve injury, which in turn permits migratory DRG neurons to acquire sympathetic characteristics. In our studies, TH^+ migratory DRG neurons maintain their dorsal axons. This could potentially allow them to interact with DRG neurons located within the ganglia, setting up a pathway for abnormal activation of pain neurons within the DRG. Further studies are needed to determine whether transdifferentiated DRG neurons play a role in neuropathic pain.

The unexpected plasticity of differentiated DRG neurons in vivo motivates future study of the possibility of a plastically differentiated state in other mature neurons that arise from multipotent precursors. In addition, our results point to plastically differentiated neurons as a novel strategy for treatment of disease and injury, and a possible mechanism for nervous system disease.

Acknowledgements
We thank Hitoshi Okamoto, Uwe Strähle and ZIRC (NIH-NRCC P40 RR012546) for providing transgenic and mutant lines; the Tubingen 2000 Screen Consortium; and members of the Ribera group for discussion. The work was supported by the National Institutes of Health [DC006880 (W.M. and T.N.); NS061409 (M.A.W.); NS039837 (M.A.W. and A.B.R.; NS048154 (A.B.R.)] and the HHMI (W.M. and T.N.). Deposited in PMC for release after 6 months.

Competing interests statement
The authors declare no competing financial interests.

Supplementary material
Supplementary material for this article is available at
http://dev.biologists.org/lookup/suppl/doi:10.1242/dev.052696/-/DC1

References

An, M., Luo, R. and Henion, P. (2002). Differentiation and maturation of zebrafish dorsal root and sympathetic ganglion neurons. *J. Comp. Neurol.* **446**, 267-275.
Blader, P., Plessy, C. and Strähle, U. (2003). Multiple regulatory elements with spatially and temporally distinct activities control neurogenin1 expression in primary neurons of the zebrafish embryo. *Mech. Dev.* **120**, 211-218.
Borodinsky, L. N., Root, C. M., Cronin, J. A., Sann, S. B., Gu, X. and Spitzer, N. C. (2004). Activity-dependent homeostatic specification of transmitter expression in embryonic neurons. *Nature* **429**, 523-530.
Carney, T., Dutton, K., Greenhill, E., Delfino-Machin, M., Dufourcq, P., Blader, P. and Kelsh, R. (2006). A direct role for Sox10 in specification of neural crest-derived sensory neurons. *Development* **133**, 4619-4630.
Chien, S. Q., Li, C., Li, H., Xie, W., Pablo, C. S. and Zhang, J. M. (2005). Sympathetic fiber sprouting in chronically compressed dorsal root ganglia without peripheral axotomy. *J. Neuropathic Pain Symptom Palliation* **1**, 19-23.
Chung, K. and Chung, J. (2001). Sympathetic sprouting in the dorsal root ganglion after spinal nerve ligation: evidence of regenerative collateral sprouting. *Brain Res.* **895**, 204-212.
Delree, P., Ribbens, C., Martin, D., Rogister, B., Lefebvre, P. P., Rigo, J. M., Leprince, P., Schoenen, J. and Moonen, G. (1993). Plasticity of developing and adult dorsal root ganglion neurons as revealed in vitro. *Brain Res. Bull.* **30**, 231-237.
Duff, R. S., Langtimm, C. J., Richardson, M. K. and Sieber-Blum, M. (1991). In vitro clonal analysis of progenitor cell patterns in dorsal root and sympathetic ganglia of the quail embryo. *Dev. Biol.* **147**, 451-459.
Dupin, E., Glavieux, C., Vaigot, P. and Le Douarin, N. M. (2000). Endothelin 3 induces the reversion of melanocytes to glia through a neural crest-derived glial-melanocytic progenitor. *Proc. Natl. Acad. Sci. USA* **97**, 7882-7887.
Dupin, E., Real, C., Glavieux-Pardanaud, C., Vaigot, P. and Le Douarin, N. M. (2003). Reversal of developmental restrictions in neural crest lineages: transition from Schwann cells to glial-melanocytic precursors in vitro. *Proc. Natl. Acad. Sci. USA* **100**, 5229-5233.
Fein, A., Wright, M., Slat, E., Ribera, A. and Isom, L. (2008). scn1bb, a zebrafish ortholog of SCN1B expressed in excitable and nonexcitable cells, affects motor neuron axon morphology and touch sensitivity. *J. Neurosci.* **28**, 12510-12522.
Fields, R. D., Neale, E. A. and Nelson, P. G. (1990). Effects of patterned electrical activity on neurite outgrowth from mouse sensory neurons. *J. Neurosci.* **10**, 2950-2964.
Gilmour, D., Maischein, H. and Nüsslein-Volhard, C. (2002). Migration and function of a glial subtype in the vertebrate peripheral nervous system. *Neuron* **34**, 577-588.
Golling, G., Amsterdam, A., Sun, Z., Antonelli, M., Maldonado, E., Chen, W., Burgess, S., Haldi, M., Artzt, K., Farrington, S. et al. (2002). Insertional mutagenesis in zebrafish rapidly identifies genes essential for early vertebrate development. *Nat. Genet.* **31**, 135-140.
Gurdon, J. B., Lemaire, P. and Kato, K. (1993). Community effects and related phenomena in development. *Cell* **75**, 831-834.
Halloran, M. and Berndt, J. (2003). Current progress in neural crest motility and migration and future prospects for the zebrafish model system. *Dev. Dyn.* **228**, 497-513.
Hanson, M. G. and Landmesser, L. T. (2004). Normal patterns of spontaneous activity are required for correct motor axon guidance and the expression of specific guidance molecules. *Neuron* **43**, 687-701.
Itoh, K., Ozaki, M., Stevens, B. and Fields, R. (1997). Activity-dependent regulation of N-cadherin in DRG neurons: differential regulation of N-cadherin, NCAM, and L1 by distinct patterns of action potentials. *J. Neurobiol.* **33**, 735-748.
Jee, M. K., Kim, J. H., Han, Y. M., Jung, S. J., Kang, K. S., Kim, D. W. and Kang, S. K. (2010). DHP-derivative and low oxygen tension effectively induces human adipose stromal cell reprogramming. *PLoS ONE* **5**, e9026.
Kanazawa, H., Ieda, M., Kimura, K., Arai, T., Kawaguchi-Manabe, H., Matsuhashi, T., Endo, J., Sano, M., Kawakami, T., Kimura, T. et al. (2010). Heart failure causes cholinergic transdifferentiation of cardiac sympathetic nerves via gp130-signaling cytokines in rodents. *J. Clin. Invest.* **120**, 408-421.
Kim, H., Na, H., Sung, B., Nam, H., Chung, Y. and Hong, S. (1999). Is sympathetic sprouting in the dorsal root ganglia responsible for the production of neuropathic pain in a rat model? *Neurosci. Lett.* **269**, 103-106.
LaBonne, C. and Bronner-Fraser, M. (1998). Induction and patterning of the neural crest, a stem cell-like precursor population. *J. Neurobiol.* **36**, 175-189.
Le Douarin, N. M. and Dupin, E. (2003). Multipotentiality of the neural crest. *Curr. Opin. Genet. Dev.* **13**, 529-536.
Lu, J., Herrera, P. L., Carreira, C., Bonnavion, R., Seigne, C., Calender, A., Bertolino, P. and Zhang, C. X. (2010). alpha-cell-specific Men1 ablation triggers the transdifferentiation of glucagon-expressing cells and insulinoma development. *Gastroenterology* **138**, 1954-1965.
Malhotra, J. D., Kazen-Gillespie, K., Hortsch, M. and Isom, L. L. (2000). Sodium channel beta subunits mediate homophilic cell adhesion and recruit ankyrin to points of cell-cell contact. *J. Biol. Chem.* **275**, 11383-11388.
McDearmid, J. R., Liao, M. and Drapeau, P. (2006). Glycine receptors regulate interneuron differentiation during spinal network development. *Proc. Natl. Acad. Sci. USA* **103**, 9679-9684.
McEwen, D. P. and Isom, L. (2004). Heterophilic interactions of sodium channel beta1 subunits with axonal and glial cell adhesion molecules. *J. Biol. Chem.* **279**, 52744-52752.
McGraw, H. F., Nechiporuk, A. and Raible, D. W. (2008). Zebrafish dorsal root ganglia neural precursor cells adopt a glial fate in the absence of neurogenin1. *J. Neurosci.* **28**, 12558-12569.
Meisler, M. H., Plummer, N. W., Burgess, D. L., Buchner, D. A. and Sprunger, L. K. (2004). Allelic mutations of the sodium channel SCN8A reveal multiple cellular and physiological functions. *Genetica* **122**, 37-45.
Nasevicius, A. and Ekker, S. C. (2000). Effective targeted gene 'knockdown' in zebrafish. *Nat. Genet.* **26**, 216-220.
Nicolson, T., Rüsch, A., Friedrich, R. W., Granato, M., Ruppersberg, J. P. and Nüsslein-Volhard, C. (1998). Genetic analysis of vertebrate sensory hair cell mechanosensation: the zebrafish circler mutants. *Neuron* **20**, 271-283.
Paulsen, N. and Matsumoto, S. G. (2000). Progenitor cells with the capacity to differentiate into sympathetic-like neurons are transiently detected in mammalian embryonic dorsal root ganglia. *J. Neurobiol.* **43**, 31-39.
Persson, A. K., Thun, J., Xu, X. J., Wiesenfeld-Hallin, Z., Strom, M., Devor, M., Lidman, O. and Fried, K. (2009). Autotomy behavior correlates with the DRG and spinal expression of sodium channels in inbred mouse strains. *Brain Res.* **1285**, 1-13.
Pineda, R., Heiser, R. and Ribera, A. (2005). Developmental, molecular, and genetic dissection of I Na in vivo in embryonic zebrafish sensory neurons. *J. Neurophysiol.* **93**, 3582-3593.
Pineda, R., Svoboda, K., Wright, M., Taylor, A., Novak, A., Gamse, J., Eisen, J. and Ribera, A. (2006). Knockdown of Nav 1.6a Na^+ channels affects zebrafish motoneuron development. *Development* **133**, 3827-3836.
Raible, D. and Eisen, J. S. (1994). Restriction of neural crest cell fate in the trunk of the embryonic zebrafish. *Development* **120**, 495-503.
Raible, D. and Eisen, J. S. (1996). Regulative interactions in zebrafish neural crest. *Development* **122**, 501-507.
Raible, D. W., Wood, A., Hodsdon, W., Henion, P. D., Weston, J. A. and Eisen, J. S. (1992). Segregation and early dispersal of neural crest cells in the embryonic zebrafish. *Dev. Dyn.* **195**, 29-42.

Rizvi, T. A., Huang, Y., Sidani, A., Atit, R., Largaespada, D. A., Boissy, R. E. and Ratner, N. (2002). A novel cytokine pathway suppresses glial cell melanogenesis after injury to adult nerve. *J. Neurosci.* **22**, 9831-9340.
Roberson, D. W., Alosi, J. A. and Cotanche, D. A. (2004). Direct transdifferentiation gives rise to the earliest new hair cells in regenerating avian auditory epithelium. *J. Neurosci. Res.* **78**, 461-471.
Sato, T., Takahoko, M. and Okamoto, H. (2006). HuC:Kaede, a useful tool to label neural morphologies in networks in vivo. *Genesis* **44**, 136-142.
Shang, J., Cafaro, J., Nehmer, R. and Stone, J. (2010). Supporting cell division is not required for regeneration of auditory hair cells after ototoxic injury in vitro. *J. Assoc. Res. Otolaryngol.* **11**, 203-222.
Shinder, V., Govrin-Lippmann, R., Cohen, S., Belenky, M., Ilin, P., Fried, K., Wilkinson, H. A. and Devor, M. (1999). Structural basis of sympathetic-sensory coupling in rat and human dorsal root ganglia following peripheral nerve injury. *J. Neurocytol.* **28**, 743-761.
Sommer, L. (2001). Context-dependent regulation of fate decisions in multipotent progenitor cells of the peripheral nervous system. *Cell Tissue Res.* **305**, 211-216.
Stevens, B., Tanner, S. and Fields, R. (1998). Control of myelination by specific patterns of neural impulses. *J. Neurosci.* **18**, 9303-9311.
Svoboda, K., Linares, A. and Ribera, A. (2001). Activity regulates programmed cell death of zebrafish Rohon-Beard neurons. *Development* **128**, 3511-3520.
Westerfield, M. (1995). *The Zebrafish Book.* Eugene: The University of Oregon Press.
Xue, Z. G. and Smith, J. (1988). High-affinity uptake of noradrenaline in quail dorsal root ganglion cells that express tyrosine hydroxylase immunoreactivity in vitro. *J. Neurosci.* **8**, 806-813.
Xue, Z. G., Smith, J. and Le Douarin, N. M. (1985). Differentiation of catecholaminergic cells in cultures of embryonic avian sensory ganglia. *Proc. Natl. Acad. Sci. USA* **82**, 8800-8804.
Xue, Z. G., Smith, J. and Le Douarin, N. M. (1987). Developmental capacities of avian embryonic dorsal root ganglion cells: neuropeptides and tyrosine hydroxylase in dissociated cell cultures. *Brain Res.* **431**, 99-109.
Yin, S., Cen, L., Wang, C., Zhao, G., Sun, J., Liu, W., Cao, Y. and Cui, L. (2010). Chondrogenic transdifferentiation of human dermal fibroblasts stimulated with cartilage derived morphogenetic protein1. *Tissue Eng. A* **16**, 1633-1643.
Yoshii, C., Ueda, Y., Okamoto, M. and Araki, M. (2007). Neural retinal regeneration in the anuran amphibian Xenopus laevis post-metamorphosis: transdifferentiation of retinal pigmented epithelium regenerates the neural retina. *Dev. Biol.* **303**, 45-56.
Zhang, J. and Strong, J. (2008). Recent evidence for activity-dependent initiation of sympathetic sprouting and neuropathic pain. *Sheng li xue bao: Acta Physiologica Sinica* **60**, 617-627.